LIVERPOOL JOHN MOORES UNIVERSITY

LJMU Research Online

Muller, AG, Sarker, SD, Fatokun, AA and Hutcheon, GA

Formulation of resveratrol into PGA-co-PDL nanoparticles increases its cytotoxic potency against lung cancer cells

https://researchonline.ljmu.ac.uk/id/eprint/18111/

Article

For more information please contact researchonline@ljmu.ac.uk

Formulation of resveratrol into PGA-co-PDL nanoparticles increases its cytotoxic potency against lung cancer cells

Ashley G. Muller[1], Satyajit D. Sarker[2], Amos A. Fatokun[2,*], [ID] and Gillian A. Hutcheon[1], [ID]

[1]School of Pharmacy and Biomolecular Sciences, Liverpool John Moores University, Liverpool, UK
[2]Centre for Natural Products Discovery (CNPD), School of Pharmacy and Biomolecular Sciences, Liverpool John Moores University, Liverpool, UK

*Correspondence: Amos A. Fatokun, Centre for Natural Products Discovery (CNPD), School of Pharmacy and Biomolecular Sciences, Liverpool John Moores University, James Parsons Building, Byrom Street, Liverpool L3 3AF, UK. Tel.: +44(0) 151 904 6291; Email: A.A.Fatokun@ljmu.ac.uk

ABSTRACT

Objectives: Lung cancer is the commonest cause of cancer-related deaths, and current treatment involves the use of cytotoxic drugs that have many unwanted side effects. Resveratrol, a natural polyphenol, has promising anticancer efficacy, but its therapeutic application is hindered by low bioavailability, which the present study sought to improve through encapsulation into nanoparticles (NPs).

Methods: Resveratrol was loaded into poly(glycerol adipate-co-ω-pentadecalactone) (PGA-co-PDL; MWt 16.5 KDa) NPs with sizes 220–230 nm, and tested against Calu-3 human lung cancer cells.

Key findings: About 5% and 10% resveratrol nanoparticles (RNPs) had a high encapsulation efficiency of 78 ± 0.24% and 70 ± 0.89% and a drug loading of 39 ± 0.12 µg and 70 ± 0.89 µg (w/w), respectively. The PGA-co-PDL blank NP (BNP) at 1 mg/ml had good cytocompatibility when Calu-3 cells were exposed to it for 24 h (cell viability of 87.5 ± 4.7%). Remarkably, the 5% RNP and 10% RNP lowered, up to 80%, the IC_{50} for 24 h cytotoxicity of resveratrol against the cells, from 158 ± 16 µM to 32 ± 10 µM and 70 ± 13 µM, respectively.

Conclusions: Loading of resveratrol into PGA-co-PDL NPs increases its anticancer potency, thus enhancing its prospect for treating lung cancer.

Keywords: biodegradable polymer(s); Cancer; cell culture; cell line(s); encapsulation; lung drug delivery; nanoparticle(s); natural product(s); polymeric drug delivery system(s); toxicity

Introduction

In the year 1878, malignant lung tumours were only 1% of all cancers identified during autopsies, as documented at the Institute of Pathology at the University of Dresden in Germany.[1, 2] After 40 years, the number increased to almost 10% and a further decade later it increased to 14%.[1] While just 374 cases of lung cancer were reported in 1912,[3, 4] by 2018, there were more than 2 million new cases of lung cancer annually, globally.[5]

There are 47 800 new cases of lung cancer every year in the UK, associated with 35 300 deaths annually from lung cancer.[6] While being the third most common cancer in the UK (13% of all new cases in 2017), lung cancer is the most common cause of death from cancer (21% of cancer deaths in 2017).[6] In the UK, 1 in 13 (8%) males and 1 in 15 (7%) females are likely to have lung cancer in their lifetime.[6] With 60% of all newly diagnosed malignant tumours and 70% of all cancer mortalities occurring amongst individuals 65 years or above, age is reckoned as the most significant risk factor for developing cancer.[7, 8] Global demographic data shows the median life expectancy is increasing, with a consequent rise in the incidence of cancer.[7, 9–11] Inevitably, therefore, incidence of and mortality from cancer will yet increase, which raises concerns about the potential scale of its further negative impact on the society, including on the economy.

In treating advanced stages of lung cancer, chemotherapy is considered the first line. It involves administering cytotoxic drugs to kill cells that have a high rate of proliferation and regeneration,[12] but with this approach it is not only cancer cells that are affected but also non-cancer cells that are rapidly dividing, for example, hair matrix cells, skin cells, epithelium cells of the mouth and gastrointestinal tract, and haematopoietic cells of the bone marrow.

Interestingly, resveratrol (*trans*-3,5,4′-trihydroxystilbene),the most common natural stilbene that is abundant in many fruits and vegetables, especially grapes,[13] possesses anti-inflammatory, anti-oxidative, pro-apoptotic and cell-cycle arrest properties.[14, 15] A systematic review revealed that, in animal models and *in vitro* cancer cell lines, resveratrol compared to a control group inferred a relative risk reduction of 0.64 (*P* = 0.002) for tumour incidence.[16]

The effects of resveratrol on lung cancer, both *in vitro* and *in vivo*, suggest that it has potential to be a treatment for cancer, although a major drawback is the low bioavailability that it (as a BCS class II drug) exhibits. While it is relatively highly absorbed orally (at least 70% absorbed), it has low oral bioavailability,[17, 18] which is perhaps as a result of its rapid sulphate conjugation by the liver or intestine.[17, 18] It is rapidly metabolised into several forms that retain some biological activity, including resveratrol 3-O-glucuronide, resveratrol 4-O-glucuronide and resveratrol trisulphate.[19, 20]

Many human studies have shown that when approximately 25 mg resveratrol was administered orally, its free form had blood plasma concentration between 1 and 5 ng/ml.[21–24] Resveratrol seems well tolerated, even at very high concentrations, with minimal side effects.[25] There is, therefore, tremendous potential for resveratrol as an anticancer agent, as evident in preclinical studies, but this has yet to be fully realised in clinical trials.[26–28] As the major issue is resveratrol's low oral bioavailability, the focus should be on improving its pharmacokinetic profile.[18] One way to realise this by using nanoparticulate drug delivery systems to aid resveratrol's efficient transport to the site of action.

Nanoparticles (NPs) and liposomes can be used to overcome the pharmacokinetic profiles of poor absorption and rapid metabolism and elimination found with most natural products. Resveratrol-loaded cationic liposomes with an encapsulation efficiency of 78.14 ± 8.04% showed a higher cellular uptake and improved anticancer activity, including significant decreases in hepatocyte nodules and liver marker enzymes compared to free resveratrol in HepG2 human liver cancer cell line.[29] Polymeric NPs are colloidal systems, spherical or irregular, that encapsulate or entrap a biologically active substance.[30] Their advantages include controllable physico-chemical properties, high stability, homogeneous size distribution, high drug encapsulation and controllable drug release.[31, 32] The therapeutic agents can be delivered through adsorption, encapsulation or conjugation, whether internally or on the surface of the polymeric NPs.[33] Several biodegradable polymers, whether synthetic and natural, could be used to formulate NPs, including poly(d,l-lactic-co-glycolic acid) (PLGA), poly(d,l -lactic acid) (PLA), poly(ε-caprolactone) (PCL), chitosan and gelatine.[34] Our group has investigated PGA-co-PDL NPs for the delivery of proteins and vaccines.[35, 36] Recently, fluorescence and confocal microscopy was used to show microRNA 146a (miR-146a) when adsorbed onto PGA-co-PDL NPs was internalised by the A549 cell line.[37] The miR-146a delivered using the PGA-co-PDL NPs retained its biological activity reducing IL-1 receptor-associated kinase expression to 40%.[37] Pneumococcal surface protein A from clade 4 (PspA4Pro) adsorbed PGA-co-PDL NPs was formulated into nanocomposite microparticles (NCMPs) for mucosal delivery targeting the lungs of mice against pneumonia.[38] The PspA4Pro containing NCMPs induced anti-PspA4Pro IgG antibodies in the serum and lungs of the mice.[38]

The study reported herein describes the formulation of resveratrol-loaded PGA-co-PDL NPs for improved cytotoxic potency. The NPs were investigated for anticancer (cytotoxic) effects in cultured Calu-3 lung cancer cells *in vitro* using cell viability and cell death assays.

Materials and Methods

Divinyl adipate (DVA) and ω-pentadecalactone (PDL) were sourced from TCI, USA and Sigma-Aldrich Fine Chemicals (SAFC, UK), respectively. Glycerol, lipase acrylic resin (previously Novozyme 435), polyvinyl alcohol (PVA) – molecular weight (MWt) 89,000–98 000, trans-resveratrol (≥99% (HPLC) were sourced from the bushy knotweed root), and the polystyrene standards (2430–29 300 Da) were sourced from Sigma-Aldrich, UK. Dichloromethane (DCM), methanol (HPLC grade) and Tetrahydrofuran (THF) were procured from Fisher Scientific, UK. L-glutamine, foetal bovine serum (FBS), Minimum Essential Medium Eagle (MEM), Penicillin-Streptomycin, resazurin sodium salt and sodium pyruvate solution were from Sigma-Aldrich, UK. Phosphate-buffered saline (PBS) and TrypLE 1× were sourced from Thermo Fisher Scientific, UK. Calu-3 (Human lung adenocarcinoma cell line) was bought from the American Type Culture Collection (ATCC). Alamar Blue and LDH assay kits were from Fisher Scientific, UK.

Synthesis of the polymer

The synthesis of PGA-co-PDL was through enzyme-(Novozyme 435) catalysed ring opening polymerisation and polycondensation as mentioned in a previous paper,[39] but with slight modifications (Figure 1). Briefly, DVA (0.125 mol), glycerol (0.125 mol) and PDL (0.125 mol) in an equimolar ratio (1:1:1) were allowed to react in THF before Novozyme 435 (1 g) was added. The reaction was permitted to continue for 6.5 h. Afterwards, DCM (200 ml) was added, and Buchner filtration was used to remove the enzyme. Rotary evaporation was employed to remove the solvent. Methanol (100 ml) was used to precipitate the polymer out of the solution and wash out any low molecular weight material (including unreacted monomers). The solid polymer was filtered and left to air dry before storage over molecular sieves. The resultant polyester was characterised using gel permeation chromatography (GPC) (Viscotek TDAModel 300 with OmniSEC5.1 software), previously calibrated using the polystyrene standards kit obtained from Supelco, USA; Fourier Transform Infra-Red spectroscopy (FT-IR; Cary 630 FT-IR Spectrometer with Agilent Technologies MicroLab FT-IR software, Agilent, USA), Proton nuclear magnetic resonance spectroscopy (¹H NMR; Bruker Avance III 300 MHz spectrometer operated with Topspin v3.2), and Differential Scanning Calorimetry (DSC) (Perkin Elmer DSC 8000 with Pyris software).

Preparation of resveratrol-loaded PGA-co-PDL nanoparticles

About 5% w/w (2.5 mg resveratrol in 50 mg PGA-co-PDL polymer) and 10% w/w (5 mg resveratrol in 50 mg PGA-co-PDL polymer) polymeric NPs encapsulated with resveratrol (5% RNP and 10% RNP) were made through a modified water-in-oil-in water ($w_1/o/w_2$) double emulsion evaporation method. PGA-co-PDL (50 mg) and resveratrol (2.5 or 5 mg) were placed in a vial together and DCM (2 ml) together with an ultrasonic water bath (Ultrawave) for 2 min was used to mix the contents. Afterwards, the solution was probe-sonicated at 65% amplitude for 2 min (QSonica sonicator, USA) while adding dropwise the first aqueous solution (10%, w/v PVA; 0.5 ml) forming an emulsion. The procedure was done on ice. The procedure was repeated with this primary emulsion while adding dropwise the second aqueous solution (1%, w/v PVA; 20 ml), forming second emulsion. Afterwards, the emulsion was transferred to a beaker and stirred at 500 rpm using a magnetic stirrer (Jeio Tech MS-53M; Jeiotech, South Korea). After 3 h, the DCM evaporated and collection of the nanoparticle suspensions was done using ultracentrifugation (Beckman Coulter Optima XPN-80), the parameters of which were: 70.1 Ti rotor spinning at 35 000 rpm for 40 min with a temperature set at 4°C. Deionised water (dH₂O) was used to rinse the NPs and the ultracentrifugation was repeated after the addition of fresh dH₂O (5ml).

Figure 1 Synthesis (enzymatic) of the PGA-co-PDL polymer via ring opening polymerisation and polycondensation.

Three batches of each formulation were prepared for evaluation and the same procedure was followed to produce blank PGA-co-PDL NPs (BNPs), except that resveratrol was not included.

Assessment of particle size and zeta potential

To assess the particle size, zeta potential and polydispersity index (PDI), dynamic light scattering with a particle size analyser (Zetasizer Nano ZS, Malvern Instruments Ltd, UK) was used. Before ultracentrifugation, an aliquot of the nanoparticle suspension (100 µl) was diluted in dH_2O (5 ml), poured into a cuvette, and measured at 25°C. The same measurements were performed on the NPs obtained after ultracentrifugation. Distilled H_2O (5 ml) was added to the NPs (10 mg) and mixed via an ultrasonic water bath (Ultrawave, UK) for 1 min. dH_2O (5 ml) was added to an aliquot (500 µl) of the suspension, transferred into a cuvette and measured.

The short-term stability of the NPs in water was assessed at 4°C and 37°C by comparing the particle size, PDI and zeta potential over a 14-day period. About 4°C was selected to mimic storage conditions and 37°C to match the physiological temperatures used in cell culture.

Assessment of drug loading and encapsulation efficiency

Each of the PGA-co-PDL NPs (BNP, 5% RNP, 10% RNP) was centrifuged to form a pellet. The pellet containing the NP was suspended in dH_2O (5 ml) and added to a 5ml screw top vials (Agilent Technologies, USA) and frozen using liquid nitrogen. The vial containing the solid mass was placed inside and lyophilised overnight using a Telstar Lyoquest Freeze-drier connected with a Telstar bomba Torricelli vacuum pump (Azbil Telstar, UK), after which it was collected and weighed.

To determine the amount of resveratrol encapsulated in the PGA-co-PDL NPs, high performance liquid chromatography (HPLC) (1200 series; Agilent Technologies, USA) using a YMC-Triart C18 150 × 4.6 mm I.D. S-5 µm, 12 nm column (YMC Co. Ltd., Japan) was employed. The lyophilised NPs (BNP, 5% RNP and 10% RNP; 10 mg) were dispersed in DCM (2 ml) in order to burst the particles. The DCM was allowed to evaporate and the mobile phase, methanol:water (51:49; v/v) (2.5 ml), was added. A plastic syringe fitted with a Captiva Econofilter PTFE 13 mm 0.45 µm filter (Agilent Technologies, USA) was used to filter the solutions (4 mg/ml) into clean 2 ml crimp vials (Agilent Technologies, USA). The injection volume of each sample was 10 µl, the flow rate was 0.54 ml/min, and the variable wavelength detector (VWD; Agilent Technologies, USA) was set to 306 nm. This method was adapted from a previously published validated method[40] and BNP was used as a control. Using these parameters, a retention time of 10.346 min and a peak width of 0.6859 min were obtained.

Resveratrol standards (0.3–62.5 µg/ml) were previously run on the HPLC (same parameters as above), with the resulting area under the curve plotted against the concentrations to obtain a calibration curve ($R2 = 0.9981$; LOD = 0.2 µg/ml; LOQ = 0.6 µg/ml) that was used to calculate the amount of resveratrol that was encapsulated into the polymeric NPs.

To calculate the theoretical drug loading (TDL), the following equation was used:

$$TDL = \frac{\text{Weight of resveratrol (mg) added}}{\text{weight of polymer(mg)}} \quad (1)$$

For 5% RNP, $(TDL) = \dfrac{2.5 \text{ mg}}{50 \text{ mg}} = 0.05 \text{ mg} = 50 \text{ } \mu g/mg \text{ (w/w)}$

For 10% RNP, $(\text{TDL}) = \dfrac{5\text{ mg}}{50\text{ mg}} = 0.1\text{ mg} = 100\ \mu\text{g/mg (w/w)}$

EE% was calculated as follows:

$$\text{EE \%} = \frac{\text{Drug loading calculated from standard curve }(\mu g)}{\text{TDL }(\mu g)} \times 100 \tag{2}.$$

In vitro release profile

The method used was adapted from a previously established method.[41] A sample (10 mg) of each of the NPs (BNP, 5% RNP, and 10 %RNP) was put in a separate, sealed Falcon tube containing PBS (10 ml; pH 7.4). A 2 ml aliquot (1 mg/ml) was then introduced into a fresh Eppendorf tube. The Eppendorf tubes (3 × 5) were put on a Grant-Bio PTR-35 multi-function rotator (Grant Instruments, UK) stirring at 30 rpm in a Stuart S160 incubator (Stuart Equipment, UK) at 37°C. At specific intervals, an Eppendorf tube per formulation was taken and centrifuged at 12 000 rpm for 10 min via an Eppendorf 5415 D centrifuge (Eppendorf, Germany). HPLC was then used to analyse the supernatant for resveratrol content as described in the 'drug loading and encapsulation efficiency' section.

Percentage resveratrol released (RR) was thus calculated as:

$$\text{RR \%} = \frac{\text{resveratrol released at time point }(\mu g)}{\text{resveratrol loaded }(\mu g)} \times 100\text{ \%} \tag{3}.$$

Assessment of the effects of agents on cell viability and cell death

Cell culture, treatments and Alamar blue viability assay

Calu-3 human lung adenocarcinoma cells were cultured in a 75 cm^2 tissue culture flask using MEM supplemented with 10% FBS, 1% L-glutamine (2 mM), 1% penicillin-streptomycin, 1% MEM Non-essential amino acids and 1% sodium pyruvate. They were housed in a humidified incubator at 37°C and 5% CO_2.

The cytotoxicity of the PGA-co-PDL BNP, resveratrol-encapsulated NPs, and free resveratrol was assessed using resurazin sodium salt (7-Hydroxy-3H-phenoxazin-3-one-10-oxide sodium salt) (Alamar Blue). Resazurin, which in its original form is blue and non-fluorescent, becomes reduced by healthy cells to resorufin, which is pink and highly fluorescent.[42]

For the assay, following trypsinisation of the T75 cultures, trituration into a suspension of single cells and haemocytometer-assisted counting under a microscope, cells were seeded at 10^3 cells/well (100 µl/well) into a Corning 96-well, opaque, clear, flat bottom plate, which was then incubated for 48 h. Afterwards, the spent media was aspirated and swapped with fresh media (100 µl/well). Then, an aliquot (100 µl) each of BNP, 5% RNP, 10% RNP and free resveratrol, prepared in complete media (0–1 mg/ml working concentrations), was added to the wells (each treatment in triplicate), with 10% dimethyl sulfoxide (DMSO) used as a positive control for cytotoxicity. After 24 h of incubation, the wells were emptied of the media, rinsed with PBS (100 µl) and refilled with fresh media (100 µl). An aliquot (10 µl) of resazurin sodium salt solution was then added to each well,

resulting in a final resazurin concentration of 50 µg/ml, and the plate was again incubated. After 3 h, the plate was read (fluorescence intensity: excitation at 540 nm and emission at 590 nm) using a CLARIOstar plate reader (BMG Labtech, Germany). The fluorescence intensity of resazurin correlates with the number of viable cells. To determine the percentage of viable cells in each well, the average fluorescence intensity of the negative (vehicle-treated) control was taken as 100% viability, to which the average fluorescence intensity of each treatment was normalised.

Lactate dehydrogenase (LDH) release assay

We used LDH release as a surrogate for cell death induced by the various tested agents. The cells were prepared as described previously but treated with a different range of concentrations: BNP, 10% RNP, free resveratrol (18.8–300 µM) and 5% RNP (9.375–150 µM). After 48 h or 72 h incubation with the agents, the LDH assay was conducted according to the supplied protocol (Catalogue No. 88954, ThermoFisher, UK). Briefly, the lysis buffer (10 µl), as complete lysis control, and ultrapure water (10 µl), as non-lysis control, were added to separate sets of wells in triplicate. Then the plate was incubated for 45 min, after which an aliquot (25 µl) of each treated well (and of the ultrapure water wells and lysis buffer wells, representing 0% lysis and 100% lysis, respectively) was transferred to a new Falcon 96-well flat bottom plate (Corning, USA). Addition of reaction mixture (25 µl) to each sample well was followed by gentle tapping to mix the solutions, after which the plate was incubated at room temperature for 30 min, protected from light. The stop solution (25 µl) was then added, followed by gentle tapping. The absorbance at 490 nm and 680 nm was read using the CLARIOstar plate reader. Each absorbance value at 680 nm (background signal from the instrument) was subtracted from the corresponding absorbance value at 490 nm.

Data presentation, statistical analyses and potency (IC$_{50}$) calculations

Values are shown as mean ± standard error of the mean (SEM) (cell studies) or mean ± standard deviation (SD) (all other studies) of three independent experiments ($n = 3$) or as otherwise stated. GraphPad Prism 7 was used to perform the statistical analyses. To determine if any mean differences were significant, one-way analysis of variance (ANOVA) followed by Tukey's multiple comparisons test was used, with $P < 0.05$ considered statistically significant. IC$_{50}$ as a measure of potency was determined using the non-linear regression equation log (inhibitor) versus response (three parameters).

Results and Discussion

Polymer synthesis

The PGA-co-PDL polymer was a white powder, as previously shown.[43] The MWt of the polymer obtained using Gel Permeation Chromatography (GPC) was 16.5 kDa, comparable to previous reports.[35] FT-IR analysis was employed to analyse the end groups of the polymerand validate completion of the reaction and formation of the product. The spectrum revealed a trough at 3455 cm^{-1}, specifying an O–H bond, as well as a sharp peak, indicating a carbonyl stretch at 1727 cm^{-1} (Figure 2a). Furthermore, the absence of the
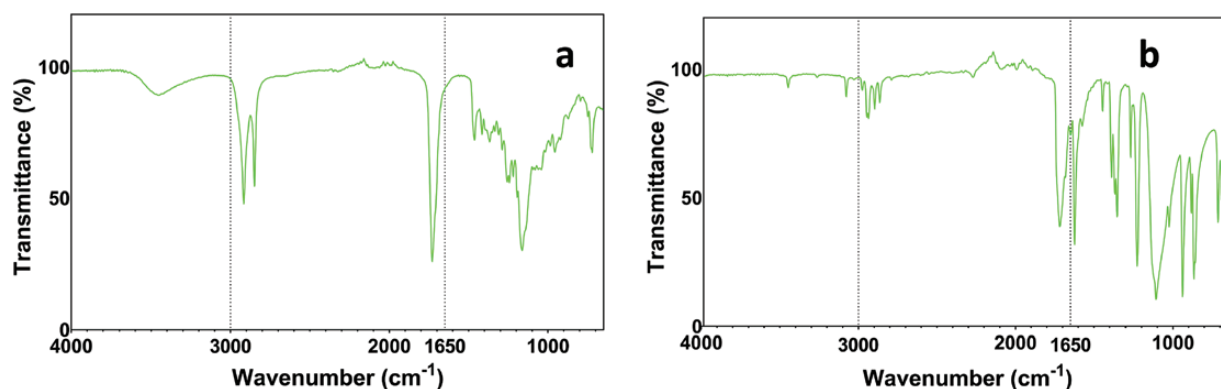
Figure 2 FT-IR spectra of (a) PGA-co-PDL and (b) DVA.

Table 1 Particle size, PDI and zeta potential of PGA-co-PDL NPs before and after centrifugation

	Before centrifugation			After centrifugation		
	BNP	5% RNP	10% RNP	BNP	5% RNP	10% RNP
Size (d.nm)	200 ± 5	205 ± 1	210 ± 5	252 ± 9	229 ± 5	221 ± 5
PDI	0.12 ± 0.04	0.14 ± 0.00	0.09 ± 0.02	0.29 ± 0.04	0.26 ± 0.03	0.22 ± 0.01
Zeta potential (mV)	*9.06 ± 0.22	−7.25 ± 0.31	−4.25 ± 0.21	−30.00 ± 1.11	−28.70 ± 0.05	−30.27 ± 0.31

Values are expressed as mean ± SD($n = 3$).
Notes: BNP, blank nanoparticles; 5% RNP, 5% resveratrol-loaded nanoparticles; 10% RNP, 10% resveratrol-loaded nanoparticles.
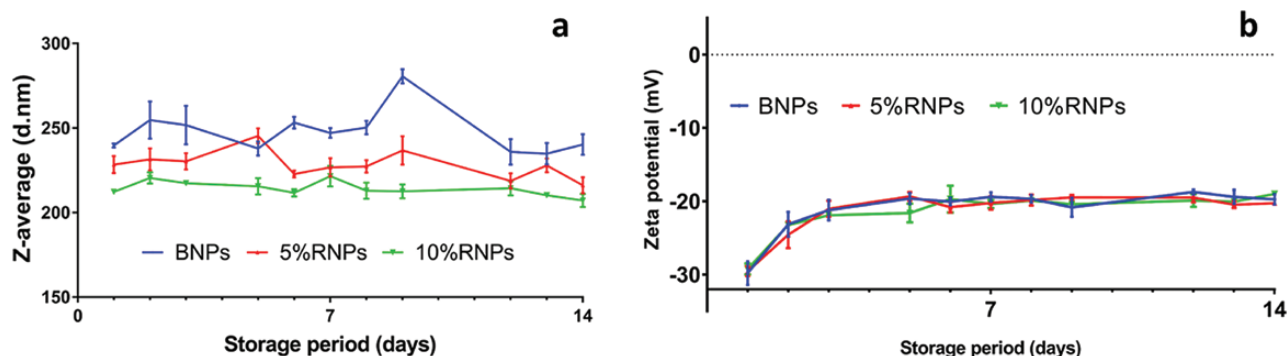
Figure 3 Effect of storage time on (a) size and (b) zeta potential of PGA-co-PDL NPs in deionised water stored at 4°C ($n = 3$).

characteristic bands associated with the terminal vinyl groups of DVA at 1650 cm⁻¹ (Figure 2b) confirmed the complete consumption of monomers during polymerisation. The integration pattern of PGA-co-PDL was confirmed by ¹H NMR spectra, ¹H NMR (300 MHz, CDCl₃) δ 4.20–3.99 (m, 6H), 2.43–2.21 (m, 6H), 1.69–1.57 (m, 8H), 1.27 (s, 22H). As determined by Differential Scanning Calorimetry (DSC), the Tm (melting point) of PGA-co-PDL was 58.5°C.

Characterisation of blank and resveratrol-loaded PGA-co-PDL nanoparticles

Resveratrol-loaded PGA-co-PDL NPs were successfully prepared via the double solvent-evaporation method. A W1/O/W2 double emulsion was used rather than a single emulsion, as previous studies have indicated the greater suitability of this method due to the increased protection offered.[44]

Table 1 summarises the particle size, PDI and zeta potential of the PGA-co-PDL NPs before and after centrifugation. Resveratrol loading does not appear to significantly influence particle size, since the particle sizes of the BNP, 5% RNP and 10% RNP did not significantly change after centrifugation. The particle size of the 5% RNP and 10% RNP (221–229 nm) was shown previously to enter A549 cells.[37] The coating of the polymers with PVA can explain the negative zeta potential obtained.[45, 46] The zeta potential of the NPs was unaffected by resveratrol, which agrees with previous studies.[47] Physical stability due to electrostatic repulsions can result from the high zeta potential (–30 mV), preventing aggregation and flocculation of the NPs.[47] There was no statistically significant change to particle size and zeta potential over a 14-day period, when stored in dH₂O at 4°C, indicating good stability of the resveratrol-loaded PGA-co-PDL NPs (Figure 3).

The encapsulation efficiencies of the 5% RNP and 10% RNP, calculated using Equations (1) and (2), were 78 ± 0.24% and 70 ± 0.89%, respectively (Figure 4a). Molecular weight, size and solubility, particle (shape and size), polymer properties (solubility, etc.), formulation processing technique and excipients are all factors that impact drug release rate.[48] A burst release was observed, with between 44% and 36% of resveratrol being immediately released from 5% RNP and 10% RNP, respectively, upon contact with the release media (Figure 4b and c), which may be due to the resveratrol on the surface of the NPs.[49, 50] Drug properties, formulation parameters, heterogeneity of matrices and percolation-limited diffusion are all factors that may produce a burst release profile.[49, 51] During formulation, not all of the drug may be encapsulated but some may rather stick to the surface of the NPs, where it is released immediately upon contact with the media.[49, 50] During a drying process, for example the freeze-drying processing of these RNPs, the water in the NPs tends to move to their surface and evaporate. Drugs may move along with water, through convection, to the surface of the nanoparticles, which could have led to burst release of resveratrol observed here.[49, 50] The maximum release obtained after 30 and 60 min was 92–99% for 5% RNP and 10% RNP, respectively. The miR-146a-adsorbed PGA-co-PDL NPs were shown to have a continuous release profile with up to 77% released after 24 h.[37] The release profile from the current study might be due to the resveratrol. Resveratrol was encapsulated into PLGA NPs and chitosan (CS)-coated PLGA NPs.[52] The PLGA NPs showed a burst release of 45.6% at 2 h, compared to only 23.9% in the CS-coated PLGA NPs at pH 7.4, but at a lower pH 5.5 the CS-coated PLGA NPs released 50% of the resveratrol at 2 h compared to 22.3% in the PLGA NPs.[52] Similarly, the release of resveratrol encapsulated in PLGA NPs was assessed at various pHs.[53] After 8 h, at pH 7.4, 6.8 and 1.2, the release of resveratrol was 29.21%, 12.49% and 10.56%, respectively.[53] This suggests the role of the pH on the release profile of resveratrol-PLGA NPs. There could be a similar mechanism involved in the PGA-co-PDL release profile; this could be investigated in the future.

Cell viability and cell death studies

In vitro effects of free resveratrol and resveratrol-loaded PGA-co-PDL NPs on cell viability

Calu-3 cells were exposed for 24 h to various concentrations of BNP, 5% RNP, 10% RNP, and free resveratrol, after which alamar blue (resazurin) was used to assess cell viability (to determine cytotoxicity). PGA-co-PDL BNP did not reduce cell viability any less than 85% of the negative control (Figure 5a), demonstrating good cytocompatibility. Similar results were found in previous studies testing PGA-co-PDL NPs/microparticles on human lung cells.[54, 55] When normal human bronchial epithelial (16HBE14o-) cells were exposed to spray-dried PGA-co-PDL microparticles, a cell viability of 87.14 ± 3.40% was obtained, even at 5 mg/ml for 24 h.[56] This lack of cytotoxic effect produced by the PGA-co-PDL NPs shows it to be a good delivery system. We established that 5% RNP, 10% RNP and free resveratrol each had a concentration-dependent cytotoxic effect on Calu-3 cells (Figure 5a–d). The IC_{50} after 24 h of exposure to the free resveratrol was 0.036 ± 0.004 mg/ml or 158 ± 16 µM (Figure 5b). Trotta *et al.* noted the insensitivity of Calu-3 cells to resveratrol, maintaining cell viability above 95% after exposure to concentrations as high as 160 µM, even after 72 h.[57] In our study, the IC_{50} for the 5% RNP and 10% RNP after 24 h treatment were 32 ± 10 µM (Figure 5c) and 70 ± 13 µM (Figure 5d), respectively, which, compared to free resveratrol, indicates a 5-fold and a 2-fold decrease in IC_{50} (or increase in potency), with a maximum percentage decrease of 80%. This result shows the effectiveness of the PGA-co-PDL NPs compared to exposing the cells to free resveratrol. The observation is similar to what has been obtained even for notable anticancer drugs, including doxorubicin and paclitaxel. For example, in a study, NPs of doxorubicin and paclitaxel caused an 8-fold and a 9-fold decrease in their respective IC_{50} values, respectively, versus the free doxorubicin and paclitaxel in human ovarian carcinoma cells.[58] Also, phenolic compounds, including quercetin, when loaded into NPs have shown an increased cytotoxic effect (decreased IC_{50}). Quercetin-encapsulated
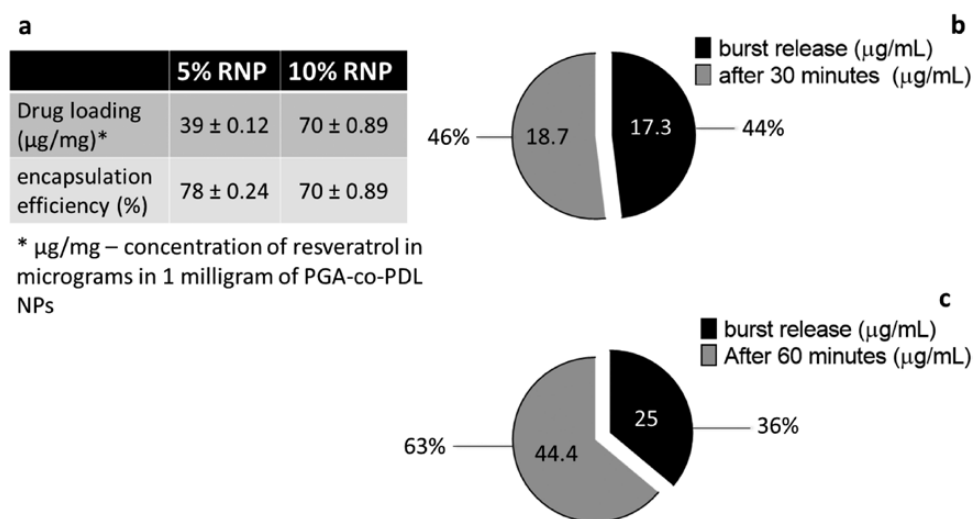
Figure 4 (a) Drug loading and encapsulation efficiency and release profiles of (b) 5% RNP and (c) 10% RNP PGA-co-PDL NPs (*n* = 3).
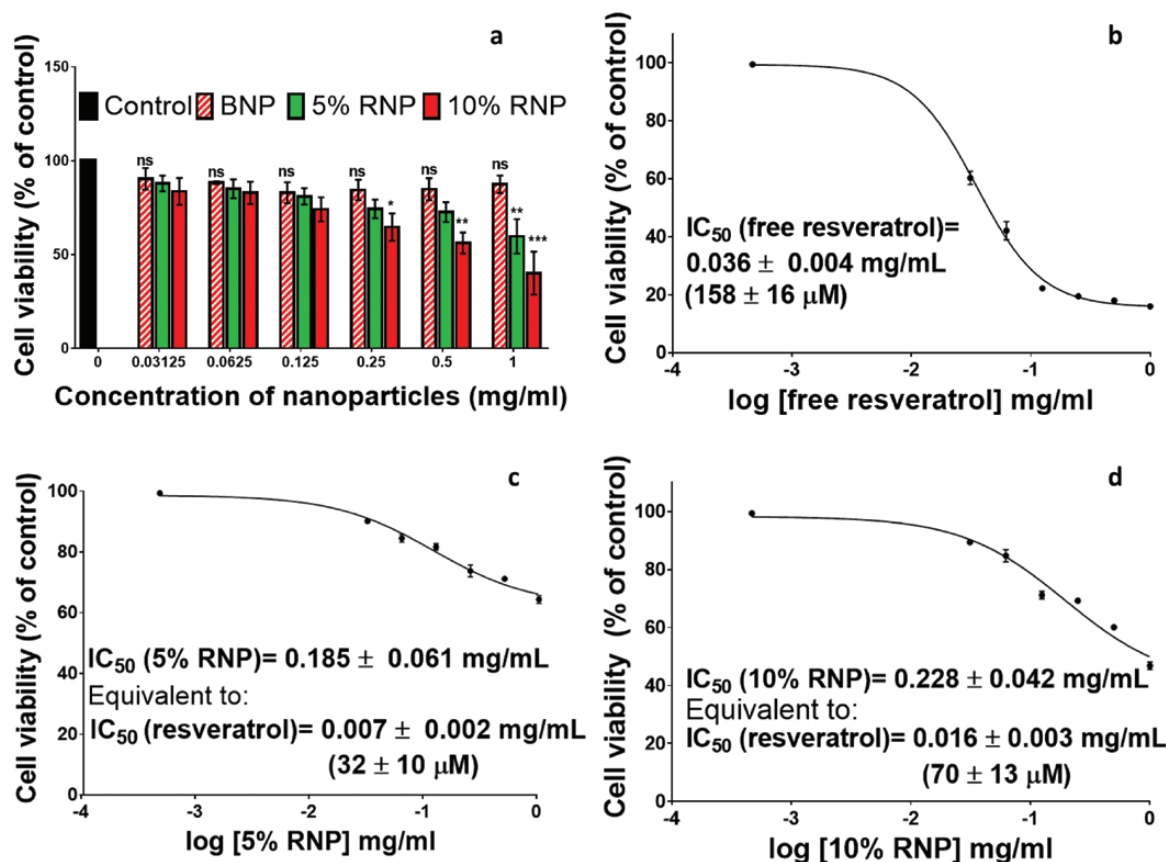
Figure 5 Effects of free resveratrol, blank nanoparticle (BNP), 5% resveratrol-loaded PGA-co-PDL nanoparticles (5% RNP) and 10% resveratrol-loaded PGA-co-PDL nanoparticles (10% RNP) on the viability of Calu-3 cells following 24 h treatment, with viability determined by the Alamar blue assay. (**a**) Lack of effect of BNP and concentration-dependent reduction of Calu-3 cell viability by RNPs; representative Log concentration-response sigmoid curves showing the effects of (b) free resveratrol, (c) 5% RNP and (d) 10% RNP. Note that 10% RNP contained 50% more resveratrol than 5% RNP. Each data point represents the mean ± SEM (n = 2). *$P < 0.05$, **$P < 0.005$, ***$P < 0.001$ and ns = not significant versus negative control.

solid lipid NPs caused a 50% decrease in IC_{50} versus free quercetin in MCF-7 cells, after 24 h.[59] Similarly, in HepG2 cells, resveratrol-encapsulated glycyrrhizic acid-conjugated human serum albumin NPs caused a 35% IC_{50} reduction after 48 h, compared to free resveratrol.[60] Furthermore, compared with free resveratrol, resveratrol-loaded gelatine NPs reduced IC_{50} by 50% after 24 h treatment of NCI-H460 non-small cell lung cancer cells.[61]

The results of the BNP versus the vehicle control did not show any statistically significant difference ($P > 0.99$) (Figure 5a), suggesting that the Calu-3 cells treated with BNP were similar, physiologically, to the cells treated with the vehicle control. These results show the promise of the BNP as a bio-compatible delivery system, implying that the resveratrol en-capsulated into the 5% RNP and 10% RNP was the cause of the cytotoxicity observed in cells treated with them. The 5% and 10% RNP each concentration-dependently reduced Calu-3 cell viability (Figure 5a). Comparing the 5% and 10% RNP to BNP showed a significant decrease in viability of cells at 1 mg/ml 5% RNP ($P < 0.005$) and for 10% BNP at 0.25 mg/ml ($P < 0.05$), 0.5 mg/ml ($P < 0.005$) and 1 mg/ml ($P < 0.001$). The concentration of polymer in BNP and 5%- and 10% RNP (all three at 1mg/ml) was equal, suggesting that the cytotoxicity caused by the RNPs was as a result of the resveratrol rather than the PGA-co-PDL NPs. It should be noted that, although the 10% RNP contained 50% more

resveratrol compared to the 5% RNP (Figure 4a), it did not have a 50% higher potency (Figure 5a). In fact, the results suggest that 5% RNP is twice as potent as 10% RNP, weight for weight (Figure 5a). The lowering of cell viability further-more suggests that, irrespective of the burst release observed, the resveratrol was effectively transported to the cells using the PGA-co-PDL NPs.

Apoptotic and necrotic cell death outcomes of the cytotoxicity induced by free resveratrol and resveratrol-loaded PGA-co-PDL NPs

LDH release was used to assess the extent of involvement of apoptosis or necrosis in the cell death induced by free resveratrol and resveratrol-loaded PGA-co-PDL NPs. For the LDH assay, no noticeable difference in LDH release was shown after 24 h (data not shown) so the cells were treated for both 48 h (Figure 6a) and 72 h (Figure 6b). To ensure an appropriate control for comparing effects, we used a 300 μM concentration of BNP, which was equivalent to the maximum concentration of polymer found in 10% RNP. 10% RNP and BNP (both at 300 μM) caused equivalent increases in the release of LDH after 48 h ($P < 0.05$) (Figure 6a), while the 10% RNP caused a much greater release of LDH compared to BNP after 72 h ($P < 0.005$) (Figure 6b). As mentioned previously, the 10% RNP and BNP (both at 300 μM) contained the same concentration of polymer, so the results suggest the
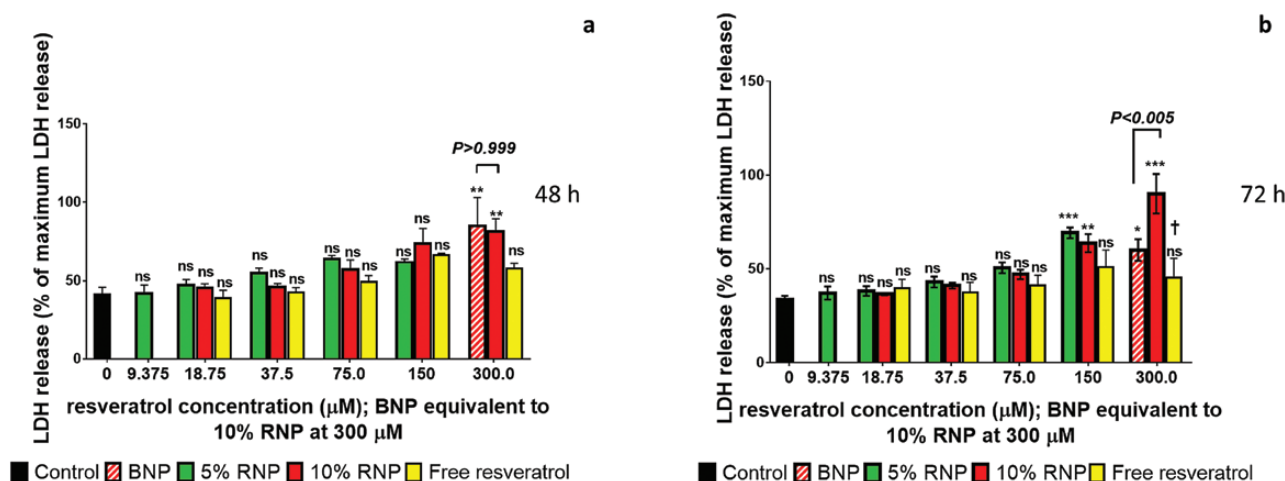
Figure 6 The effects on LDH release (indicative of cell death) in Calu-3 cells of blank PGA-co-PDL nanoparticles (BNP), 5% resveratrol-loaded PGA-co-PDL nanoparticles (5% RNP), 10% resveratrol-loaded PGA-co-PDL nanoparticles (10% RNP) and free resveratrol after treatments for (a) 48 h and (b) 72 h. Each data point represents the mean ± SEM ($n = 3$). *$P < 0.05$, ** $P < 0.005$, ***$P < 0.001$, ns = not significant versus control; and †$P < 0.001$ compared to 10% RNP 300 μM.

resveratrol encapsulated into the NP as the source of the increased LDH release. Additionally, no significant increase in the release of LDH was found between free resveratrol and the control at 48 h and 72 h ($P > 0.05$), while 300 μM 10% RNP produced a significant increase in the release of LDH versus 300 μM free resveratrol after 72 h ($P < 0.001$) (Figure 6b). These results demonstrate a significant increase in potency of the resveratrol when delivered using the PGA-co-PDL NPs. Mechanistically, time-dependent induction of late-stage apoptosis as an outcome of RNP-induced cytotoxicity was also demonstrated, as LDH release occurs as a result of compromise to the cell membrane, which is usually associated with necrosis or late-stage apoptosis. In this case, since significant LDH release was not observed until 72 h after treatment, we suspect the 10% RNP-induced LDH release probably indicated late-stage apoptosis (further mechanistic assays such as those assessing caspase activity could be carried out in the future to firmly establish apoptosis), a finding consistent with previous reports. For example, administration of resveratrol (0–100 μM) to human lung carcinoma cells (A549 and CH27) caused a concentration-dependent increase in LDH leakage[62] and resveratrol could induce cellular apoptosis. 3T3-L1 adipocytes treated with resveratrol up to 100 μM showed a concentration-dependent increase in LDH leakage, suggesting resveratrol may induce apoptosis.[63] These cells were further investigated using mitochondrial membrane potential (MMP), flow cytometry and western blotting, which revealed, respectively, a concentration-dependent decrease in MMP, a significant increase in the ratio of apoptotic cells from 5.8% to 39.6%, and an upregulation of apoptotic markers, including cleaved caspase 3.[63] Similarly, treatment of the human SCLC H446 cell line with 40 μg/ml resveratrol led to inhibition of cell viability and induction of apoptosis, assessed via MTT assay and flow cytometry, respectively.[64] Studies show that resveratrol encapsulated in nanoparticles retains these properties. Elgizawy et al. (2021)[65] formulated resveratrol encapsulated, chitosan-coated, nanostructured lipid carriers (CSNLCs), which were shown to possess the ability to induce apoptosis through activation of caspase-3

and the death receptor. These properties make resveratrol suitable as an anticancer compound. Taken together, our results demonstrate that the encapsulation of resveratrol PGA-co-PDL NPs reduces the viability of Calu-3 cells and induces apoptotic cell death in a concentration- and time-dependent manner. However, while the work is a proof of concept for enhancing resveratrol potency, for pulmonary delivery, the resveratrol-encapsulated NPs would require spray-drying to form nanocomposite microparticles.[66–68]

Conclusion

The results demonstrate successful encapsulation of resveratrol into PGA-co-PDL NPs with high efficiency. The PGA-co-PDL-encapsulated resveratrol was shown to be much more potent than free resveratrol in decreasing the viability of (or eliciting cytotoxicity in) lung cancer cells and inducing their apoptosis. These results highlight that this is a very promising approach for enhancing the potency of resveratrol or similar agents through the use of PGA-co-PDL or related nanoparticles, hence inspiring further research in this area.

Ethical Information

The research reported in this paper did not require ethical permission.

Author Contributions

Ashley G. Muller: conceptualisation, methodology, validation, formal analysis, data curation, investigation, writing – original draft, writing – review and editing, visualisation and funding acquisition. Satyajit D. Sarker: conceptualisation, methodology, resources, writing – review and editing, supervision and project administration. Amos A. Fatokun: conceptualisation, methodology, validation, formal analysis, investigation, resources, writing – review and editing, visualisation, supervision and project administration. Gillian

A. Hutcheon: conceptualisation, methodology, validation, formal analysis, resources, writing – review and editing, visualisation, funding acquisition, supervision and project administration. All authors read and approved the manuscript.

Conflicts of Interest

The authors declare that there are no conflicts of interest

Data Availability Statement

The data that support the findings of this study are available from the corresponding authors upon reasonable request.

References

1. Witschi H. A short history of lung cancer. *Toxicol Sci* 2001; 64: 4–6. https://doi.org/10.1093/toxsci/64.1.4
2. Semenova EA, Nagel R, Berns A. Origins, genetic landscape, and emerging therapies of small cell lung cancer. *Genes Dev* 2015; 29: 1447–62. https://doi.org/10.1101/gad.263145.115
3. Spiro SG, Silvestri GA. One hundred years of lung cancer. *Am J Respir Crit Care Med* 2005; 172: 523–9. https://doi.org/10.1164/rccm.200504-531OE
4. Ong P, Ost D. Lung cancer epidemiologic changes: implications in diagnosis and therapy. In: Díaz-Jimenez J, Rodriguez A, (eds). Interventions in Pulmonary Medicine. Springer, Cham; 2017; 323–32. https://doi.org/10.1007/978-3-319-58036-4_20
5. International Agency for Research on Cancer. *Globocan 2018*. 2018. http://gco.iarc.fr/today (10 March 2019, last date accessed).
6. Cancer Research UK. *Lung Cancer Statistics*. 2020. https://www.cancerresearchuk.org/health-professional/cancer-statistics/statistics-by-cancer-type/lung-cancer#heading-One (20 March 2020, last date accessed).
7. Al-Mansour Z, Pang L, Bathini V. Novel cancer therapeutics in geriatrics: what is unique to the aging patient? *Drugs Aging* 2019; 36: 1–11. https://doi.org/10.1007/s40266-018-0619-2
8. Smith BD, Hurria A, Buchholz TA et al. Future of cancer incidence in the United States: burdens upon an aging, changing nation. *J Clin Oncol* 2009; 27: 2758–65. https://doi.org/10.1200/JCO.2008.20.8983
9. Pilleron S, Sarfati D, Janssen-Heijnen M et al. Global cancer incidence in older adults, 2012 and 2035: a population-based study. *Int J Cancer* 2018; 144: 49–58. https://doi.org/10.1002/ijc.31664.
10. Torre LA, Siegel RL, Ward EM et al. Global cancer incidence and mortality rates and trends-an update. *Cancer Epidemiol Biomarkers Prev.* 2016; 25: 16–27. https://doi.org/10.1158/1055-9965.EPI-15-0578.
11. Bray F, Ferlay J, Soerjomataram I et al. Global cancer statistics 2018: GLOBOCAN estimates of incidence and mortality worldwide for 36 cancers in 185 countries. *CA Cancer J Clin* 2018; 68: 394–424. https://doi.org/10.3322/caac.21492
12. Feitelson MA, Arzumanyan A, Kulathinal RJ et al. Sustained proliferation in cancer: mechanisms and novel therapeutic targets. *Semin Cancer Biol* 2015; 35: S25–54. https://doi.org/10.1016/j.semcancer.2015.02.006
13. Francioso A, Mastromarino P, Restignoli R et al. Improved stability of trans-resveratrol in aqueous solutions by carboxymethylated (1,3/1,6)-beta-d-glucan. *J Agric Food Chem* 2014; 62: 1520–5. https://doi.org/10.1021/jf404155e
14. Yu X-D, Yang J, Zhang W-L et al. Resveratrol inhibits oral squamous cell carcinoma through induction of apoptosis and G2/M phase cell cycle arrest. *Tumor Biol* 2016; 37: 2871–7. https://doi.org/10.1007/s13277-015-3793-4
15. Albuquerque RV, Malcher NS, Amado LL et al. In vitro protective effect and antioxidant mechanism of resveratrol induced by dapsone hydroxylamine in human cells. *PLoS One* 2015; 10. https://doi.org/10.1371/journal.pone.0134768
16. Feng Y, Zhou J, Jiang Y. Resveratrol in lung cancer – a systematic review. *J BUON* 2016; 21: 950–3.
17. Walle T, Hsieh F, Delegge MH et al. High absorption but very low bioavailability of oral resveratrol in humans. *Drug Metab Dispos* 2004; 32: 1377–82. https://doi.org/10.1124/dmd.104.000885
18. Chimento A, De Amicis F, Sirianni R et al. Progress to improve oral bioavailability and beneficial effects of resveratrol. *Int J Mol Sci* 2019; 20: 1381. https://doi.org/10.3390/ijms20061381
19. Gambini J, Inglés M, Olaso G et al. Properties of resveratrol: in vitro and in vivo studies about metabolism, bioavailability, and biological effects in animal models and humans. *Oxid Med Cell Longev* 2015; 2015: 1–13. https://doi.org/10.1155/2015/837042
20. Wang P, Sang S. Metabolism and pharmacokinetics of resveratrol and pterostilbene. *BioFactors* 2018; 44: 16–25. https://doi.org/10.1002/biof.1410
21. Soleas GJ, Yan Y, Goldberg DM. Measurement of trans-resveratrol,(+)-catechin, and quercetin in rat and human blood and urine by gas chromatography with mass selective detection. In: Packer L (Ed.), *Methods Enzymol*. San Diego: Elsevier, 2001, 130–145.
22. Soleas GJ, Yan J, Goldberg DM. Ultrasensitive assay for three polyphenols (catechin, quercetin and resveratrol) and their conjugates in biological fluids utilizing gas chromatography with mass selective detection. *J Chromatogr B Biomed Sci Appl* 2001; 757: 161–72. https://doi.org/10.1016/s0378-4347(01)00142-6
23. Almeida L, Vaz-da-Silva M, Falcão A et al. Pharmacokinetic and safety profile of trans-resveratrol in a rising multiple-dose study in healthy volunteers. *Mol Nutr Food Res* 2009; 53: S7–15. https://doi.org/10.1002/mnfr.200800177
24. Loira-Pastoriza C, Todoroff J, Vanbever R. Delivery strategies for sustained drug release in the lungs. *Adv Drug Deliv Rev* 2014; 75: 81–91. https://doi.org/10.1016/j.addr.2014.05.017
25. Patel KR, Scott E, Brown VA et al. Clinical trials of resveratrol. *Ann N Y Acad Sci* 2011; 1215: 161–9. https://doi.org/10.1111/j.1749-6632.2010.05853.x
26. Tomé-Carneiro J, Larrosa M, González-Sarrías A et al. Resveratrol and clinical trials: the crossroad from in vitro studies to human evidence. *Curr Pharm Des* 2013; 19: 6064–93. https://www.ingentaconnect.com/content/ben/cpd/2013/00000019/00000034/art00003?crawler=true&mimetype=application/pdf (accessed 26 June 2019).
27. Borriello A, Bencivenga D, Caldarelli I et al. Resveratrol: from basic studies to bedside. *Cancer Treat Res* 2014; 159: 167–84. https://doi.org/10.1007/978-3-642-38007-5_10
28. Singh CK, Ndiaye MA, Ahmad N. Resveratrol and cancer: challenges for clinical translation. *Biochim Biophys Acta Mol Basis Dis* 2015; 1852: 1178–85. https://doi.org/10.1016/J.BBADIS.2014.11.004
29. Jagwani S, Jalalpure S, Dhamecha D et al. Pharmacokinetic and pharmacodynamic evaluation of resveratrol loaded cationic liposomes for targeting hepatocellular carcinoma. *ACS Biomater Sci Eng* 2020; 6: 4969–84. https://doi.org/10.1021/acsbiomaterials.0c00429
30. Vittorio O, Curcio M, Cojoc M et al. Polyphenols delivery by polymeric materials: challenges in cancer treatment. *Drug Deliv* 2017; 24: 162–80. https://doi.org/10.1080/10717544.2016.1236846

31. Hu CMJ, Aryal S, Zhang L. Nanoparticle-assisted combination therapies for effective cancer treatment. *Ther Deliv* 2010; 1: 323–34. https://doi.org/10.4155/tde.10.13

32. Farooq MA, Aquib M, Khan DH et al. Nanocarrier-mediated co-delivery systems for lung cancer therapy: recent developments and prospects. *Environ Chem Lett* 2019; 17: 1–19. https://doi.org/10.1007/s10311-019-00897-7

33. Ahmadi Z, Mohammadinejad R, Ashrafizadeh M. Drug delivery systems for resveratrol, a non-flavonoid polyphenol: emerging evidence in last decades. *J Drug Deliv Sci Technol* 2019; 51: 591–604. https://doi.org/10.1016/j.jddst.2019.03.017

34. Kumari A, Yadav SK, Yadav SC. Biodegradable polymeric nanoparticles based drug delivery systems. *Colloids Surf B Biointerfaces* 2010; 75: 1–18. https://www.sciencedirect.com/science/article/pii/S0927776509004111 (18 July 2018, last date accessed).

35. Alfagih I, Kunda N, Alanazi F et al. Pulmonary delivery of proteins using nanocomposite microcarriers. *J Pharm Sci* 2015; 104: 4386–98. https://doi.org/10.1002/jps.24681

36. Kunda NK, Alfagih IM, Miyaji EN et al. Pulmonary dry powder vaccine of pneumococcal antigen loaded nanoparticles. *Int J Pharm* 2015; 495: 903–12. https://doi.org/10.1016/j.ijpharm.2015.09.034

37. Mohamed A, Kunda NK, Ross K et al. Polymeric nanoparticles for the delivery of miRNA to treat Chronic Obstructive Pulmonary Disease (COPD). *Eur J Pharm Biopharm* 2019; 136: 1–8. https://doi.org/10.1016/j.ejpb.2019.01.002

38. Rodrigues TC, Oliveira MLS, Soares-Schanoski A et al. Mucosal immunization with PspA (pneumococcal surface protein A)-adsorbed nanoparticles targeting the lungs for protection against pneumococcal infection. *PLoS One* 2018; 13: e0191692. https://doi.org/10.1371/journal.pone.0191692

39. Tawfeek HM, Evans AR, Iftikhar A et al. Dry powder inhalation of macromolecules using novel PEG-co-polyester microparticle carriers. *Int J Pharm* 2013; 441: 611–9. https://doi.org/10.1016/j.ijpharm.2012.10.036

40. da Rocha Lindner G, Khalil NM, Mainardes RM. Resveratrol-loaded polymeric nanoparticles: validation of an HPLC-PDA method to determine the drug entrapment and evaluation of its antioxidant activity resveratrol-loaded polymeric nanoparticles: validation of an HPLC-PDA method to determine the drug E. *Sci World J* 2013; 2013: 506083. https://doi.org/10.1155/2013/506083

41. Li J, Zhao L, Huang X et al. Polyethyleneglycol-modified poly(*d, l*-lactideco-glycolide) loaded resveratrol nanoparticles characterization and their anti-cancer activities. *J Nanosci Nanotechnol* 2016; 16: 9477–81. https://doi.org/10.1166/jnn.2016.12368

42. O'Brien J, Wilson I, Orton T et al. Investigation of the Alamar Blue (resazurin) fluorescent dye for the assessment of mammalian cell cytotoxicity. *Eur Biochem Soc J* 2000; 267: 5421–6. http://www.ncbi.nlm.nih.gov/pubmed/10951200

43. Thompson CJ, Hansford D, Higgins S et al. Enzymatic synthesis and evaluation of new novel ω-pentadecalactone polymers for the production of biodegradable microspheres. *J Microencapsul* 2006; 23: 213–26. https://doi.org/10.1080/02652040500444123

44. Wang J, Shi A, Agyei D et al. Formulation of water-in-oil-in-water (W/O/W) emulsions containing trans-resveratrol. *RSC Adv* 2017; 7: 35917–27. https://doi.org/10.1039/c7ra05945k

45. Ranjan AP, Zeglam K, Mukerjee A, Thamake S, Vishwanatha JK. A sustained release formulation of chitosan modified PLCL: poloxamer blend nanoparticles loaded with optical agent for animal imaging. *Nanotechnology*. 2011; 22. https://doi.org/10.1088/0957-4484/22/29/295104

46. Shagholani H, Ghoreishi SM, Mousazadeh M. Improvement of interaction between PVA and chitosan via magnetite nanoparticles for drug delivery application, *Int J Biol Macromol*. 2015; 78: 130–6. https://doi.org/10.1016/j.ijbiomac.2015.02.042

47. Neves AR, Martins S, Segundo MA, Reis S. Nanoscale delivery of resveratrol towards enhancement of supplements and nutraceuticals. *Nutrients*. 2016; 8. https://doi.org/10.3390/nu8030131

48. Varma MVS, Kaushal AM, Garg A et al. Factors affecting mechanism and kinetics of drug release from matrix-based oral controlled drug delivery systems. *Am J Drug Deliv* 2004; 2: 43–57. https://doi.org/10.2165/00137696-200402010-00003

49. Huang X, Brazel CS. On the importance and mechanisms of burst release in matrix-controlled drug delivery systems. *J Control Release* 2001; 73: 121–36. https://doi.org/10.1016/s0168-3659(01)00248-6

50. Kamaly N, Yameen B, Wu J et al. Degradable controlled-release polymers and polymeric nanoparticles: mechanisms of controlling drug release. *Chem Rev* 2016; 116: 2602–63. https://doi.org/10.1021/acs.chemrev.5b00346

51. Peppas NA, Narasimhan B. Mathematical models in drug delivery: how modeling has shaped the way we design new drug delivery systems. *J Control Release* 2014; 190: 75–81. https://doi.org/10.1016/j.jconrel.2014.06.041

52. Aldawsari HM, Alhakamy NA, Padder R et al. Preparation and characterization of chitosan coated plga nanoparticles of resveratrol: improved stability, antioxidant and apoptotic activities in H1299 lung cancer cells. *Coatings* 2020; 10. https://doi.org/10.3390/coatings10050439

53. Wan S, Zhang L, Quan Y et al. Resveratrol-loaded PLGA nanoparticles: enhanced stability, solubility and bioactivity of resveratrol for non-alcoholic fatty liver disease therapy. *R Soc Open Sci* 2018; 5. https://doi.org/10.1098/rsos.181457.

54. Kunda NK. *Dry Powder Inhalation of Pneumococcal Vaccine Using Polymeric Nanoparticles as Carriers*. Liverpool John Moores University, 2014.

55. Tawfeek H, Khidr S, Samy E et al. Poly(Glycerol Adipate-co-ω-Pentadecalactone) spray-dried microparticles as sustained release carriers for pulmonary delivery. *Pharm Res* 2011; 28: 2086–97. https://doi.org/10.1007/s11095-011-0433-6

56. Tawfeek HM. Evaluation of PEG and mPEG-co-(PGA-co-PDL) microparticles loaded with sodium diclofenac. *Saudi Pharm J* 2013; 21: 387–97. https://doi.org/10.1016/j.jsps.2012.11.006

57. Trotta V, Lee W-H, Loo C-Y et al. In vitro biological activity of resveratrol using a novel inhalable resveratrol spray-dried formulation. *Int J Pharm* 2015; 491: 190–7. https://doi.org/10.1016/j.ijpharm.2015.06.033

58. Dong X, Mattingly CA, Tseng MT et al. Doxorubicin and paclitaxel-loaded lipid-based nanoparticles overcome multidrug resistance by inhibiting P-glycoprotein and depleting ATP. *Cancer Res* 2009; 69: 3918–26. https://doi.org/10.1158/0008-5472.CAN-08-2747

59. Niazvand F, Orazizadeh M, Khorsandi L et al. Effects of Quercetin-loaded nanoparticles on MCF-7 human breast cancer cells. *Med* 2019; 55: 1–15. https://doi.org/10.3390/medicina55040114

60. Wu M, Lian B, Deng Y et al. Resveratrol-loaded glycyrrhizic acid-conjugated human serum albumin nanoparticles wrapping resveratrol nanoparticles: preparation, characterization, and targeting effect on liver tumors. *J Biomater Appl* 2017; 32: 191–205. https://doi.org/10.1177/0885328217713357

61. Karthikeyan S, Rajendra Prasad N, Ganamani A et al. Anticancer activity of resveratrol-loaded gelatin nanoparticles on NCI-H460 non-small cell lung cancer cells. *Biomed Prev Nutr* 2013; 3: 64–73. https://doi.org/10.1016/J.BIONUT.2012.10.009.

62. Weng CJ, Yang YT, Ho CT et al. Mechanisms of apoptotic effects induced by resveratrol, dibenzoylmethane, and their analogues on human lung carcinoma cells. *J Agric Food Chem* 2009; 57: 5235–43. https://doi.org/10.1021/jf900531m

63. Chen S, Zhou N, Zhang Z et al. Resveratrol induces cell apoptosis in adipocytes via AMPK activation. *Biochem Biophys Res Commun* 2015; 457: 608–13. https://doi.org/10.1016/j.bbrc.2015.01.034

64. Li W, Li C, Ma L et al. Resveratrol inhibits viability and induces apoptosis in the small-cell lung cancer H446 cell line via the PI3K/Akt/c-Myc pathway. *Oncol Rep* 2020; 44: 1821–30. https://doi.org/10.3892/or.2020.7747

65. Elgizawy HA, Ali AA, Hussein MA. Resveratrol: isolation, and its nanostructured lipid carriers, inhibits cell proliferation, induces cell

apoptosis in certain human cell lines carcinoma and exerts protective effect against paraquat-induced hepatotoxicity. *J Med Food* 2021; 24: 89–100. https://doi.org/10.1089/jmf.2019.0286

66. Rezazadeh M, Davatsaz Z, Emami J et al. Preparation and characterization of spray-dried inhalable powders containing polymeric micelles for pulmonary delivery of paclitaxel in lung cancer. *J Pharm Pharm Sci* 2018; 21: 200. https://doi.org/10.18433/jpps30048

67. Elsayed I, AbouGhaly MHH. Inhalable nanocomposite microparticles: preparation, characterization and factors affecting formulation. *Expert Opin Drug Deliv* 2016; 13: 207–22. https://doi.org/10.1517/17425247.2016.1102224

68. Kunda NK, Alfagih IM, Dennison SR et al. bovine serum albumin adsorbed PGA-co-PDL nanocarriers for vaccine delivery via dry powder inhalation. *Pharm Res* 2015; 32: 1341–53. https://doi.org/10.1007/s11095-014-1538-5